

The genome and transcriptome of the *Phalaenopsis* yield insights into floral organ development and flowering regulation

Jian-Zhi Huang, Chih-Peng Lin, Ting-Chi Cheng, Ya-Wen Huang, Yi-Jung Tsai, Shu-Yun Cheng, Yi-Wen Chen, Chueh-Pai Lee, Wan-Chia Chung, Bill Chia-Han Chang, Shih-Wen Chin, Chen-Yu Lee, Fure-Chyi Chen

Phalaenopsis orchid is an important potted flower with high economic value around the world. We report the 3.1 Gb draft genome assembly of an important winter flowering *Phalaenopsis* 'KHM190' cultivar. We generated 89.5 Gb RNA-seq and 113 million sRNA-seq reads to use these data to identify 41,153 protein-coding genes and 188 miRNA families. We also generated a draft genome for *Phalaenopsis pulcherrima* 'B8802', a summer flowering species, via resequencing. Comparison of genome data between the two *Phalaenopsis* cultivars allowed the identification of 691,532 single-nucleotide polymorphisms. In this study, we reveal the key role of *PhAGL6b* in the regulation of labellum organ development involves alternative splicing in big lip mutant. Petal or sepal overexpressing *PhAGL6b* lead to the conversion into lip-like structure. We also evidenced the gibberellin pathway that regulates the expression of flowering time genes during the reproductive phase change induced by cool temperature. Our work thus depicted a valuable resource for the flowering control, flower architecture development, and breeding of the *Phalaenopsis* orchids.

1 **The genome and transcriptome of the *Phalaenopsis* yield insights into floral**
2 **organ development and flowering regulation**

3

4 Jian-Zhi Huang^{1*}, Chih-Peng Lin^{2,4*}, Ting-Chi Cheng¹, Ya-Wen Huang¹, Yi-Jung Tsai¹, Shu-Yun
5 Cheng¹, Yi-Wen Chen¹, Chueh-Pai Lee², Wan-Chia Chung², Bill Chia-Han Chang^{2,3#}, Shih-Wen
6 Chin^{1#}, Chen-Yu Lee^{1#} & Fure-Chyi Chen^{1#}

7

8

9 ¹Department of Plant Industry, National Pingtung University of Science and Technology,
10 Pingtung 91201, Taiwan

11 ²Yourgene Bioscience, Shu-Lin District, New Taipei City 23863, Taiwan

12 ³Faculty of Veterinary Science, The University of Melbourne, Parkville Victoria 3010 Australia

13 ⁴Department of Biotechnology, School of Health Technology, Ming Chuan University, Gui Shan
14 District, Taoyuan 333, Taiwan

15

16

17 *These authors contributed equally to this work.

18 #Correspondence should be addressed to B-C.H.C. (bchang@yourgene.com.tw), S.-W.C.
19 (swchin@mail.npust.edu.tw), C.-Y.L. (culee@mail.npust.edu.tw) & F.-C.C.
20 (fchen@mail.npust.edu.tw)

21

22

23

24

25

26

27

28

29

30

31

32

33

34

35 Abstract

36 *Phalaenopsis* orchid is an important potted flower with high economic value around
37 the world. We report the 3.1 Gb draft genome assembly of an important winter flowering
38 *Phalaenopsis* ‘KHM190’ cultivar. We generated 89.5 Gb RNA-seq and 113 million sRNA-
39 seq reads to use these data to identify 41,153 protein-coding genes and 188 miRNA families.
40 We also generated a draft genome for *Phalaenopsis pulcherrima* ‘B8802’, a summer
41 flowering species, via resequencing. Comparison of genome data between the two
42 *Phalaenopsis* cultivars allowed the identification of 691,532 single-nucleotide
43 polymorphisms. In this study, we reveal the key role of *PhAGL6b* in the regulation of
44 labellum organ development involves alternative splicing in big lip mutant. Petal or sepal
45 overexpressing *PhAGL6b* lead to the conversion into lip-like structure. We also evidenced
46 the gibberellin pathway that regulates the expression of flowering time genes during the
47 reproductive phase change induced by cool temperature. Our work thus depicted a valuable
48 resource for the flowering control, flower architecture development, and breeding of the
49 *Phalaenopsis* orchids.

50

51

52

53

54

55

56

57

58

59

60

61

62

63

64

65

66

67

68

69

70

71

72 1. Introduction

73 *Phalaenopsis* is a genus within the family Orchidaceae and comprises approximately 66
74 species distributed throughout tropical Asia (Christenson 2002). The predicted *Phalaenopsis*
75 genome size is approximately 1.5 gigabases (Gb), which is distributed across 19 chromosomes
76 (Lin et al. 2001). *Phalaenopsis* flowers have a zygomorphic floral structure, including three
77 sepals (in the first floral whorl), two petals and the third petal develops into a labellum in early
78 stage of development, which is a distinctive feature of a highly modified floral part in second
79 floral whorl unique to orchids. The gynostemium contains the male and female reproductive
80 organs in the center (Rudall & Bateman 2002). In the ABCDE model, B-class genes play
81 important role to perianth development in orchid species (Chang et al. 2010; Mondragon-
82 Palomino & Theissen 2011; Tsai et al. 2004). In addition, *PhAGL6a* and *PhAGL6b*, expressed
83 specifically in the *Phalaenopsis* labellum, were implied to play as a positive regulator of labellum
84 formation (Huang et al. 2015; Su et al. 2013). However, the relationship between the function of
85 genes involved in floral-organ development and morphological features remains poorly
86 understood.

87 *Phalaenopsis* orchids are produced in large quantity annually and are traded as the most
88 important potted plants worldwide. During greenhouse production of young plants, the high
89 temperature $>28^{\circ}\text{C}$ was routinely used to promote vegetative growth and inhibit spike initiation
90 (Blanchard & Runkle 2006). Conversely, a lower ambient temperature ($24/18^{\circ}\text{C}$ day/night) is
91 used to induce spiking (Chen et al. 2008) to produce flowering plants. Spike induction in
92 *Phalaenopsis* orchid by this cool temperature is the key to precisely control its flowering date.
93 Several studies have indicated that cool temperature during the night are necessary for
94 *Phalaenopsis* orchids to flower (Blanchard & Runkle 2006; Chen et al. 1994; Chen et al. 2008;
95 Wang 1995). Despite a number of expressed sequence tags (ESTs), RNA-seqs and sRNA-seqs
96 from several tissues of *Phalaenopsis* have been reported and deposited in GenBank or OrchidBase
97 (An & Chan 2012; An et al. 2011; Hsiao et al. 2011; Su et al. 2011), only a few flowering related
98 genes or miRNAs have been identified and characterized. Besides, the clues to the spike initiation
99 during reproductive phase change in the shorten stem, which may produce signals related to
100 flowering during cool temperature induction, have not been dealt with. So far, the molecular
101 mechanisms leading to spiking of *Phalaenopsis* has yet to be elucidated.

102 Here we report a high-quality genome and transcriptomes (mRNAs and small RNAs) of
103 *Phalaenopsis* Brother Spring Dancer ‘KHM190’, a winter flowering hybrid with spike formation
104 in response to low temperature. We also provide resequencing data for summer flowering species
105 *P. pulcherrima* ‘P8802’. Our comprehensive genomic and transcriptome analyses provide
106 valuable insights into the molecular mechanisms of important biological processes such as floral
107 organ development and flowering time regulation.

108

109 2. METHODS SUMMARY

110 The genome of the *Phalaenopsis* Brother Spring Dancer ‘KHM190’ cultivar was sequenced on
111 the Illumina HiSeq 2000 platform. The obtained data were used to assemble a draft genome
112 sequence using the Velvet software (Zerbino & Birney 2008). RNA-Seq and sRNA-Seq data
113 were generated on the same platform for genome annotation and transcriptome and small RNA
114 analyses. Repetitive elements were identified by combining information on sequence similarity at
115 the nucleotide and protein levels and by using de novo approaches. Gene models were predicted
116 by combining publically available *Phalaenopsis* RNA-Seq data and RNA-Seq data generated in
117 this project. RNA-Seq data were mapped to the repeat masked genome with Tophat (Trapnell et
118 al. 2009) and CuffLinks (Trapnell et al. 2012). The detailed methodology and associated
119 references are available in the SI Appendix.

120

121 3. Results and Discussion

122 **3.1 Genome sequencing and assembly.** We sequenced the genome of the *Phalaenopsis*
123 orchid cultivar ‘KHM190’ (SI Appendix, Fig. S1a) using the Illumina HiSeq 2000 platform and
124 assembled the genome with the Velvet assembler, using 300.5 Gb (90-fold coverage) of filtered
125 high-quality sequence data (SI Appendix, Table S1). This cultivar has an estimated genome size
126 of 3.45 Gb on the basis of a 17-mer depth distribution analysis of the sequenced reads (SI
127 Appendix, Fig. S2 and S3 and Table S2 and S3). *De novo* assembly of the Illumina reads resulted
128 in a sequence of 3.1 Gb, representing 89.9% of the *Phalaenopsis* orchid genome. Following gap
129 closure, the assembly consisted of 149,151 scaffolds (≥ 1000 bp), with N50 lengths of 100 kb and
130 1.5 kb for the contigs. Approximately 90% of the total sequence was covered by 6,804 scaffolds
131 of >100 kb, with the largest scaffold spanning 1.4 Mb (SI Appendix, Table S3-S5 and Dataset
132 S17). The sequencing depth of 92.5% of the assembly was more than 20 reads (SI Appendix, Fig.
133 S3), ensuring high accuracy at the nucleotide level. The GC content distribution in the
134 *Phalaenopsis* genome was comparable with that in the genomes of *Arabidopsis* (2000), *Oryza*
135 (2005) and *Vitis* (Jaillon et al. 2007) (SI Appendix, Fig. S4).

136

137 **3.2 Gene prediction and annotation.** Approximately 59.74% of the *Phalaenopsis* genome
138 assembly was identified as repetitive elements, including long terminal repeat retrotransposons
139 (33.44%), DNA transposons (2.91%) and unclassified repeats (21.99%) (SI Appendix, Fig. S5
140 and Table S6). To facilitate gene annotation, we identified 41,153 high-confidence and medium-
141 confidence protein-coding regions with complete gene structures in the *Phalaenopsis* genome
142 using RNA-Seq (114.1 Gb for a 157.6 Mb transcriptome assembly), based on 15 libraries
143 representing four tissues (young floral organs, leaves, shortened stems and protocorm-like bodies
144 (PLBs)) (SI Appendix, Table S7 and Dataset S18), and we used transcript assemblies of these
145 regions in combination with publically available expressed sequence tags (Su et al. 2011; Tsai et

146 al. 2013) for gene model prediction and validation (Dataset S1-S2). We predicted 41,153 genes
147 with an average mRNA length of 1,014 bp and a mean number of 3.83 exons per gene (Table 1
148 and Dataset S3). In addition to protein coding genes, we identified a total of 562 ribosomal
149 RNAs, 655 transfer RNAs, 290 small nucleolar RNAs and 263 small nuclear RNAs in the
150 *Phalaenopsis* genome (SI Appendix, Table S8). We also obtained 92,811,417 small RNA (sRNA)
151 reads (18-27 bp), representing 6,976,375 unique sRNA tags (SI Appendix, Fig. S6 and Dataset
152 S6-S7). A total of 650 miRNAs distributed in 188 families were identified (Dataset S8), and a
153 total of 1,644 miRNA-targeted genes were predicted through the alignment of conserved
154 miRNAs to our gene models (SI Appendix, Fig. S7 and Dataset S9-S10).

155 The *Phalaenopsis* gene families were compared with those of *Arabidopsis* (2000), *Oryza*
156 (2005), and *Vitis* (Jaillon et al. 2007) using OrthoMCL (Li et al. 2003). We identified 41,153
157 *Phalaenopsis* genes in 15,855 families, with 8,532 gene families being shared with *Arabidopsis*,
158 *Oryza* and *Vitis*. Another 5,143 families, containing 12,520 genes, were unique to *Phalaenopsis*
159 (Figure 1). In comparison with the 29,431 protein-coding genes estimated for the *Phalaenopsis*
160 *equestris* genome (Cai et al. 2015), our gene set for *Phalaenopsis* ‘KHM190’ contained 11,722
161 more members, suggesting a more wider representation of genes in this work. This difference in
162 gene number may be due to different approaches between *Phalaenopsis* ‘KHM190’ and
163 *Phalaenopsis equestris*. Besides, *Phalaenopsis* ‘KHM190’ is a hybrid while *P. equestris* species,
164 which may show gene number difference due to different genetic background. To better annotate
165 the *Phalaenopsis* genome for protein-coding genes, we generated RNA-seq reads obtained from
166 four tissues as well as publically available expressed sequence tags for cross reference. We
167 defined the function of members of these families using Gene ontology (2008), the Kyoto
168 Encyclopedia of Genes and Genomes (Kanehisa et al. 2012) and Pfam protein motifs (Finn et al.
169 2014) (Figure. 2 and Dataset S3-S5 and Dataset S19).

170 The genes in the HC (High confidence) and MC (Medium Confidence) gene sets were
171 functionally annotated based on homology to annotated genes from the NCBI non-redundant
172 database (Dataset S3). The functional domains of *Phalaenopsis* genes were identified by
173 comparing their sequences against protein databases, including the Gene Ontology (GO) (2008),
174 Kyoto Encyclopedia of Genes and Genomes (KEGG) (Kanehisa et al. 2012) and Pfam (Finn et al.
175 2014; Finn et al. 2011) databases. GO terms were obtained using the Blast2GO program (Conesa
176 & Gotz 2008). In the GO annotations, 16,034, 27,294, and 16,360 genes were assigned to the
177 biological process, cellular compound, and molecular function categories, respectively (Figure.
178 2A). Based on KEGG pathway mapping, we were able to assign a significant proportion of the
179 *Phalaenopsis* gene sets to KEGG functional or biological pathway categories (11,452 sequences;
180 140 KEGG orthologous terms) (Dataset S4). To investigate protein families, we compared the
181 Pfam domains of *Phalaenopsis* genome. A total of 1,842 Pfam domains were detected among the
182 *Phalaenopsis* sequences. The most abundant protein domains in *Phalaenopsis* genome were

183 pentatricopeptide repeats (PPRs, pfam01535), followed by the WD40 (pfam00400), EF hand
184 (pfam00036) and ERM (Ezrin/radixin/moesin, pfam00769) domains (Figure. 2B and Dataset S5).
185 Furthermore, conserved domains could be identified in 50.17% of the predicted protein sequences
186 based on comparison against Pfam databases. In addition, we identified 2,610 transcription
187 factors (6.34% of the total genes) and transcriptional regulators in 55 gene families (SI Appendix,
188 Fig. S8-S10 and Dataset S11-S12).

189

190 **3.3 Regulation of *Phalaenopsis* floral organ development.** The relative expression of all
191 *Phalaenopsis* genes was compared through RNA-Seq analysis of shoot tip tissues from shortened
192 stems, leaf, floral organs and PLB samples, in addition to vegetative tissues, reproductive tissues,
193 and germinating seeds from *P. aphrodite* (Su et al. 2011; Tsai et al. 2013) (SI Appendix, Fig. S12
194 and Dataset S1). *Phalaenopsis* orchids exhibit a unique flower morphology involving outer
195 tepals, lateral inner tepals and a particularly conspicuous labellum (lip) (Rudall & Bateman
196 2002). However, our understanding of the regulation of the floral organ development of the genus
197 is still in its infancy. To comprehensively characterize the genes involved in the development of
198 *Phalaenopsis* floral organs, we obtained RNA-Seq data for the sepals, petals and labellum of both
199 the wild-type and peloric mutant of *Phalaenopsis* ‘KHM190’ at the 0.2-cm floral bud stage, at
200 which shows early sign of labellum differentiation. This cultivar presented an early peloric fate in
201 its lateral inner tepals. In a peloric flower, the lateral inner tepals are converted into a lip-like
202 morphology at this young bud stage (SI Appendix, Fig. S12a and 11b). We identified 3,743 genes
203 that were differentially expressed in the floral organs of the wild-type and peloric mutant plants.
204 Gene Ontology analysis of the differentially expressed genes in *Phalaenopsis* floral organs
205 revealed functions related to biological regulation, developmental processes and nucleotide
206 binding, which were significantly altered in both genotypes (Huang et al. 2015). Transcription
207 factors (TFs) seem to play a role in floral organ development. Of the 3,309 putative TF genes
208 identified in the *Phalaenopsis* genome showed differences in expression between the wild-type
209 and peloric mutant plants (Dataset S11).

210 MADS-box genes are of ancient origin and are found in plants, yeasts and animals (Trobner
211 et al. 1992). This gene family can be divided into two main lineages, referred to as type I and
212 type II. Type I genes only share sequence similarity with type II genes in the MADS domain
213 (Alvarez-Buylla et al. 2000). Most of the well-studied plant genes are type II genes and contain
214 three domains that are not present in type I genes: an intervening (I) domain, a keratin-like
215 coiled-coil (K) domain, and a C-terminal (C) domain (Munster et al. 1997). These genes are best
216 known for their roles in the specification of floral organ development, the regulation of flowering
217 time and other aspects of reproductive development (Dornelas et al. 2011). In addition, MADS-
218 box genes are also widely expressed in vegetative tissues (Messenguy & Dubois 2003;
219 Parenicova et al. 2003). The ABCDE model comprises five major classes of homeotic selector

220 genes: A, B, C, D and E, most of which are MADS-box genes (Theissen 2001). However,
221 research on the ABCDE model was mainly focused on herbaceous plants and has not fully
222 explained how diverse angiosperms evolved. The function of many other genes expressed during
223 floral development remains obscure. *Phalaenopsis* exhibits unique flower morphology involving
224 three types of perianth organs: outer tepals, lateral inner tepals, and a labellum (Rudall &
225 Bateman 2002). Despite its unique floral morphological features, the molecular mechanism of
226 floral development in *Phalaenopsis* orchid remains largely unclear, and further research is needed
227 to identify genes involved in floral differentiation. Recently, several remarkable research studies
228 on *Phalaenopsis* MADS-box genes have revealed important roles of some of these genes in floral
229 development, such as four B-class *DEF*-like MADS-box genes that are differentially expressed
230 between wild-type plants and peloric mutants with lip-like petals (Tsai et al. 2004) and a *PI*-like
231 gene, *PeMADS6*, that is ubiquitously expressed in petaloid sepals, petals, columns and ovaries
232 (Tsai et al. 2005).

233 In the *Phalaenopsis* genome sequence assembly, a total of 122 genes were predicted to
234 encode MADS-box family proteins (SI Appendix, Fig. S8, Dataset S12). To obtain a more
235 accurate classification, phylogenetic trees were constructed via the neighbour-joining method,
236 with 1000 bootstraps using MEGA5 (Tamura et al. 2011).. The differentially expressed genes
237 (DEGs) among 122 *Phalaenopsis* MADS-box genes were obtained from our *Phalaenopsis* RNA-
238 Seq data (Dataset S11). The expression profile indicated that most MADS-box genes are widely
239 expressed in diverse tissues. These results will be helpful to elucidate the regulatory roles of these
240 genes in *Phalaenopsis* floral organ development.

241 Notably, we previously reported one of the MADS-box genes, *PhAGL6b*, upregulated in the
242 peloric lateral inner tepals (lip-like petals) and lip organs (Huang et al. 2015). To understand the
243 expression mode, we therefore cloned the full-length sequence of *PhAGL6b* from lip organ
244 cDNA libraries for the wild-type, peloric mutant and big lip mutant. The big lip mutant developed
245 a petaloid labellum instead of the regular lip observed in the wild-type flower (Figure 3B).
246 Interestingly, we identified firstly four alternatively spliced forms of *PhAGL6b* that were
247 specifically expressed only in the petaloid labellum of the big lip mutant (Figure 3C and 3D and
248 SI Appendix, Fig. S11). To determine whether the alternatively spliced forms of *PhAGL6b* affect
249 the conversion of the labellum to a petal-like organ in the big lip mutant, we performed RT-PCR
250 of total RNA extracted from the labellum organs of plants with different big lip mutant
251 phenotypes and wild-type plants (SI Appendix, Table S11, Figure 4A) to amplify the *PhAGL6b*
252 transcripts. Interestingly, among all of the big lip mutant phenotypes, 500~700 bp bands were
253 detected, corresponding to *PhAGL6b* alternatively spliced forms, which were not found in any of
254 the other orchid plants (Figure 4A). We further examined the expression of *PhAGL6b* and its
255 alternatively spliced forms in the labellum organs of *Phalaenopsis* plants with different big lip
256 phenotypes and wild-type plants via real-time PCR (SI Appendix, Table S11). In the big lip

257 mutants, the expression of native *PhAGL6b* was reduced by 42~70%, whereas all of the
258 alternatively spliced forms were expressed more strongly compared with the wild-type plants
259 (figure 4B). In summary, the RT-PCR and real-time PCR experiments corroborated the specific
260 expression of the alternatively spliced forms of *PhAGL6b* in the petal-like lip of big lip mutants.
261 Thus, *PhAGL6b* might play crucial role in the development of the labellum in *Phalaenopsis*.

262 The four isoforms of the encoded PhAGL6b products differ only in the length of their C-
263 terminus region (Figure 3D). C-domain is important for the activation of transcription of target
264 genes (Honma & Goto 2001) and may affect the nature of the interactions with other MADS-box
265 proteins in multimeric complexes (Geuten et al. 2006; Gramzow & Theissen 2010). In *Oncidium*,
266 L (lip) complex (OAP3-2/OAGL6-2/OAGL6-2/OPI) is required for lip formation (Hsu et al.
267 2015). The *Phalaenopsis PhAGL6b* is an orthologue of *OAGL6-2*. In our study, the PhAGL6b
268 and its different spliced forms may each other compete the *Phalaenopsis* L-like complex to affect
269 labellum development as reported in *Oncidium* (Hsu et al. 2015). This provides a novel clue
270 further supporting the notion that *PhAGL6b* may function as a key floral organ regulator in
271 *Phalaenopsis* orchids, with broad impacts on petal, sepal and labellum development (Figure 3E).

272

273 **3.4 Control of flowering time in *Phalaenopsis*.** The flowering of *Phalaenopsis* orchids is a
274 response to cues related to seasonal changes in light (Wang 1995), temperature (Blanchard &
275 Runkle 2006) and other external influences (Chen et al. 1994). A cool night temperature of 18-
276 20°C for approximately 4 weeks will generally induce spiking in most *Phalaenopsis* hybrids,
277 while high temperature inhibits it. To compare gene expression between a constant high-
278 temperature (30/27°C; day/night) and inducing cool temperature (22/18°C), we collected shoot
279 tip tissues from shortened stems of mature *P. aphrodite* plants after treatment at a constant high
280 temperature (BH) and a cool temperature (BL) (1 to 4 weeks) for RNA-Seq data analysis (SI
281 Appendix, Fig. S12g-i). More than 7,500 *Phalaenopsis* genes were found to be highly expressed
282 in the floral meristems during the 4 successive cool temperature periods (showing at least a 2-fold
283 difference in the expression level in the BL condition relative to BH) (Dataset S13). The
284 identified flowering-related genes correspond to transcription factors and genes involved in signal
285 transduction, development and metabolism (Figure 3 and Dataset S14). The classification of
286 these genes includes the following categories: photoperiod, gibberellins (GAs), ambient
287 temperature, light-quality pathways, autonomous pathways and floral pathway integrators
288 (Fornara et al. 2010; Mouradov et al. 2002). However, the genes involved in the photoperiod,
289 ambient temperature, light quality and autonomous pathways did not show significant changes in
290 the floral meristems during the cool temperature treatments (SI Appendix, Fig. S13 and Dataset
291 S14). By contrast, the expression patterns of genes involved in pathways that regulate flowering,
292 comprising a total of 22 GA pathway-related genes, were related to biosynthesis, signal
293 transduction and responsiveness. The GA pathway-related genes and the floral pathway integrator

294 genes have been revealed as representative key players in the link between flowering promotion
295 pathways and the floral transition regulation network in several plant species (Mutasa-Gottgens
296 & Hedden 2009). In contrast to the expression patterns observed in BL and BH, the GA
297 biosynthetic pathway and positively acting regulator genes showed high expression levels in BL.
298 Furthermore, the expression level of negatively acting regulators, like DELLA genes identified,
299 was suppressed by the cool temperature which allowing the activation of flowering related genes
300 . The genes included in the flowering promotion pathways and floral pathway integrators were
301 generally upregulated in BL (Figure 5 and Figure 6 and Dataset S11). These findings suggest that
302 the GA pathway may play a crucial role in the regulation of flowering time in *Phalaenopsis*
303 orchid during cool temperature.

304

305 **3.5 Genetic polymorphisms for *Phalaenopsis* orchids.** The *Phalaenopsis* genome assembly
306 also provides the basis for the development of molecular marker-assisted breeding. Analysis of
307 the *Phalaenopsis* genome revealed a total of 532,285 simple sequence repeats (SSRs) (SI
308 Appendix, Fig. S14 and Table S9 and Dataset S15). To enable the identification of single
309 nucleotide polymorphisms (SNPs), we re-sequenced the genome of a summer flowering species,
310 *P. pulcherrima* ‘B8802’, with about tenfolds coverage. Comparison of the genome data from the
311 two *Phalaenopsis* accessions (KHM190 and B8802) allowed the discovery of 691,532 SNPs,
312 which should be valuable for future development of SNP markers for *Phalaenopsis* marker-
313 assisted selection. (SI Appendix, Fig. S15 and Table S10 and Dataset S16). *P. pulcherrima* is an
314 important parent for small flower and summer-flowering cultivars in breeding program. These
315 SNP markers may contribute valuable tools for varietal identification, genetic linkage map
316 development, genetic diversity analysis, and marker-assisted selection breeding in *Phalaenopsis*
317 orchid.

318

319 **4. Conclusion**

320 In this study, we sequenced, de novo assembled, and extensively annotated the genome of one of
321 the most important *Phalaenopsis* hybrid. We also annotated the genome with a wealth of RNA-
322 seq and sRNA-seq from different tissues, and many genes and miRNAs related to floral organ
323 development, flowering time and protocorm (embryo) development were identified. Importantly,
324 this RNA-Seq and sRNA-seq data allowed us to further improve the genome annotation quality.
325 In addition, mining of SSR and SNP molecular markers from the genome and transcriptomes is
326 currently being adopted in advanced breeding programs and comparative genetic studies, which
327 should contribute to efficient *Phalaenopsis* cultivar development. Despite the *P. equestris*
328 genome has been reported recently (Cai et al. 2015), focus on floral organ development and
329 flowering time regulation has not been dealt with. In our study, we obtained transcriptomes from
330 shortened stems, which initiate spikes in response to low ambient temperature, and floral organs

331 and generated valuable data of potentially regulate flowering time key genes and floral organ
332 development. The genome and transcriptome information of our work should provide a
333 constructive reference resource to upgrade the efficiency of cultivation and genetic improvement
334 of *Phalaenopsis* orchids.

335

336

337

338

339

340

341

342

343

344 **Data deposition:**

345 The *Phalaenopsis* genome assembly, transcriptomic and sRNA-seq data were deposited in
346 Genbank with BioProject ID PRJNA271641. The version described in this paper is the first
347 version, JXCR00000000. All short-read data are available via Sequence Read Archive:
348 SRR1747138, SRR1753943, SRR1753944, SRR1753945, SRR1753946, SRR1753947,
349 SRR1753948, SRR1753949, SRR1753950, SRR1752971, SRR1753106, SRR1753165,
350 SRR1753166 (*Phalaenopsis* ‘KHM190’ genomic DNA); SRR1762751, SRR1762752,
351 SRR1762753 (*Phalaenopsis* ‘B8802’ genomic DNA); SRR1760428, SRR1760429,
352 SRR1760430, SRR1760432, SRR1760433, SRR1760435, SRR1760436, SRR1760438,
353 SRR1760439, SRX396172, SRX396784, SRX396785, SRX396786, SRX396787, SRX396788
354 (RNA-seq); SRR1760091, SRR1760211, SRR1760212, SRR1760213, SRR1760270,
355 SRR1760271, SRR1760523, SRR1760524, SRR1760525, SRR1760526, SRR1760527,
356 SRR1760528, SRR1760530, SRR1760531, SRR1760532 (small RNA)

357 **Figure Legends**

358 **Figure 1. Venn diagram showing unique and shared gene families between and among**
359 ***Phalaenopsis*, *Oryza*, *Arabidopsis* and *Vitis*.**

360

361 **Figure 2. GO (A) and Pfam (B) annotation of *Phalaenopsis* protein-coding genes.**

362

363 **Figure 3. Possible evolutionary relationship of *PhAGL6b* in the regulation of lip formation**
364 **and floral symmetry in *Phalaenopsis* orchid.**

365 (A) Wild-type flower. (B) A big lip mutant of *Phalaenopsis* World Class ‘Big Foot’. (C)
366 Representative RT-PCR result showing the mRNA splicing pattern of *PhAGL6b* in wild-type (W)
367 and big lip mutant (M). (D) Alignment of the amino acid sequences of alternatively spliced forms
368 of *PhAGL6b*. (E) Model of *PhAGL6b* spatial expression for controlling *Phalaenopsis* floral
369 symmetry. Ectopic expression of *PhAGL6b* in the distal domain (petal; pink), petal converts into
370 a lip-like structure that leads to radial symmetry. Ectopic expression in proximal domain, (sepal;
371 blue) sepal converts into a lip-like structure that leads to bilateral symmetry¹⁵. The alternative
372 processing of *PhAGL6b* transcripts produced in proximal domain (labellum; pink), labellum
373 converts into a petal-like structure that leads to radial symmetry. *PhAGL6b* expression patterns in
374 *Phalaenopsis* floral organs are either an expansion or a reduction across labellum. This implies
375 that *PhAGL6b* may be a key regulator to the bilateral or radially symmetrical evolvments. Pink
376 color: 2nd whorl of the flower; blue color: 1st whorl of the flower; fan-shaped symbol: petal or
377 petal-like structure; triangle symbol: labellum or lip-like structure; Curved symbol: sepal.

378

379 **Figure 4. Different labellum types of wild-type and big lip mutant *Phalaenopsis* flowers.** RT-
380 PCR analysis of the mRNA splicing pattern of *PhAGL6b* in wild-type plants (98201-WT1 and
381 98201-WT2) and different big lip mutant types (A). Splicing variants of *PhAGL6b*, as detected
382 via qRT-PCR in the labellum organ of different big lip mutant types (B).

383

384 **Figure 5. Expression profiles of genes of flowering time regulation pathway with high**
385 **temperature and cool temperature treatment. Only the genes with twofold change in**
386 **expression during cool temperature treatments are revealed**

387

388

389

390

391

392 **Figure 6. Predicted pathway in the regulation of spike induction in**
393 ***Phalaenopsis*.**

394 Red color indicates that the involved genes are more highly expressed in the GA biosynthesis
395 pathway; whereas pink color of gene names indicates their differential expression in the GA
396 response pathway. Blue colors of gene names represent the activation of flower
397 architecture genes. Red arrows show the steps of the GA signaling stage; Pink arrows direct the
398 steps of inflorescence evocation stage; Blue arrows reveal the steps of flower stalk initiation
399 stage. Black arrows indicate the genes downregulated 2X
400 over. *GA20ox*, *GA3ox*, *GAMYB*, *FT*, *SOC1*, *LFY* and *API* are upregulated 2X over.

401

402

403

404

405

406

407

408

409

410

411

412

413

414

415

416

417

418

419

420

421

422

423

424

425

426

427

428

429 **Supplementary files**

430

431 SUPPLEMENTARY INFORMATION APPENDIX

432 Dataset 1-14

433 Dataset 13

434 Dataset 15

435 Dataset 16

436 Dataset 17:https://drive.google.com/open?id=0B_TRDroXHRivc1MwYjJwT1ZIZVU

437 Dataset 18

438 Dataset 19

439

440

441

442

443

444

445

446

447

448

449

450

451

452

453

454

455

456

457

458

459

460

461

462

463

464

465

466

467 **REFERENCES**

- 468 2000. Analysis of the genome sequence of the flowering plant *Arabidopsis thaliana*. *Nature*
469 408:796-815. 10.1038/35048692
- 470 2005. The map-based sequence of the rice genome. *Nature* 436:793-800. 10.1038/nature03895
- 471 2008. The Gene Ontology project in 2008. *Nucleic Acids Res* 36:D440-444. 10.1093/nar/gkm883
- 472 Alvarez-Buylla ER, Pelaz S, Liljegren SJ, Gold SE, Burgeff C, Ditta GS, Ribas de Pouplana L,
473 Martinez-Castilla L, and Yanofsky MF. 2000. An ancestral MADS-box gene duplication
474 occurred before the divergence of plants and animals. *Proc Natl Acad Sci U S A* 97:5328-
475 5333.
- 476 An FM, and Chan MT. 2012. Transcriptome-wide characterization of miRNA-directed and non-
477 miRNA-directed endonucleolytic cleavage using Degradome analysis under low ambient
478 temperature in *Phalaenopsis aphrodite* subsp. *formosana*. *Plant Cell Physiol* 53:1737-
479 1750. 10.1093/pcp/pcs118
- 480 An FM, Hsiao SR, and Chan MT. 2011. Sequencing-based approaches reveal low ambient
481 temperature-responsive and tissue-specific microRNAs in *phalaenopsis* orchid. *PLoS One*
482 6:e18937. 10.1371/journal.pone.0018937
- 483 Blanchard MG, and Runkle ES. 2006. Temperature during the day, but not during the night,
484 controls flowering of *Phalaenopsis* orchids. *J Exp Bot* 57:4043-4049. 10.1093/jxb/erl176
- 485 Cai J, Liu X, Vanneste K, Proost S, Tsai WC, Liu KW, Chen LJ, He Y, Xu Q, Bian C, Zheng Z,
486 Sun F, Liu W, Hsiao YY, Pan ZJ, Hsu CC, Yang YP, Hsu YC, Chuang YC, Dievert A,
487 Dufayard JF, Xu X, Wang JY, Wang J, Xiao XJ, Zhao XM, Du R, Zhang GQ, Wang M, Su
488 YY, Xie GC, Liu GH, Li LQ, Huang LQ, Luo YB, Chen HH, Van de Peer Y, and Liu ZJ.
489 2015. The genome sequence of the orchid *Phalaenopsis equestris*. *Nat Genet* 47:65-72.
490 10.1038/ng.3149
- 491 Chang YY, Kao NH, Li JY, Hsu WH, Liang YL, Wu JW, and Yang CH. 2010. Characterization of
492 the possible roles for B class MADS box genes in regulation of perianth formation in
493 orchid. *Plant Physiol* 152:837-853. 10.1104/pp.109.147116
- 494 Chen W-S, Liu H-Y, Liu Z-H, Yang L, and Chen W-H. 1994. Geibberlin and temperature
495 influence carbohydrate content and flowering in *Phalaenopsis*. *Physiologia Plantarum*
496 90:391-395. 10.1111/j.1399-3054.1994.tb00404.x
- 497 Chen WH, Tseng YC, Liu YC, Chuo CM, Chen PT, Tseng KM, Yeh YC, Ger MJ, and Wang HL.
498 2008. Cool-night temperature induces spike emergence and affects photosynthetic
499 efficiency and metabolizable carbohydrate and organic acid pools in *Phalaenopsis*
500 *aphrodite*. *Plant Cell Rep* 27:1667-1675. 10.1007/s00299-008-0591-0
- 501 Christenson EA. 2001. *Phalaenopsis*: a monograph. Portland Oregon: Timber Press.
- 502 Conesa A, and Gotz S. 2008. Blast2GO: A comprehensive suite for functional analysis in plant
503 genomics. *Int J Plant Genomics* 2008:619832. 10.1155/2008/619832

- 504 Dornelas MC, Patreze CM, Angenent GC, and Immink RG. 2011. MADS: the missing link
505 between identity and growth? *Trends Plant Sci* 16:89-97. 10.1016/j.tplants.2010.11.003
- 506 Finn RD, Bateman A, Clements J, Coggill P, Eberhardt RY, Eddy SR, Heger A, Hetherington K,
507 Holm L, Mistry J, Sonnhammer EL, Tate J, and Punta M. 2014. Pfam: the protein families
508 database. *Nucleic Acids Res* 42:D222-230. 10.1093/nar/gkt1223
- 509 Finn RD, Clements J, and Eddy SR. 2011. HMMER web server: interactive sequence similarity
510 searching. *Nucleic Acids Res* 39:W29-37. 10.1093/nar/gkr367
- 511 Fornara F, de Montaigu A, and Coupland G. 2010. SnapShot: Control of flowering in
512 *Arabidopsis*. *Cell* 141:550, 550 e551-552. 10.1016/j.cell.2010.04.024
- 513 Geuten K, Becker A, Kaufmann K, Caris P, Janssens S, Viaene T, Theissen G, and Smets E. 2006.
514 Petaloidy and petal identity MADS-box genes in the balsaminoid genera *Impatiens* and
515 *Marcgravia*. *Plant J* 47:501-518. 10.1111/j.1365-313X.2006.02800.x
- 516 Gramzow L, and Theissen G. 2010. A hitchhiker's guide to the MADS world of plants. *Genome*
517 *Biol* 11:214. 10.1186/gb-2010-11-6-214
- 518 Honma T, and Goto K. 2001. Complexes of MADS-box proteins are sufficient to convert leaves
519 into floral organs. *Nature* 409:525-529. 10.1038/35054083
- 520 Hsiao YY, Chen YW, Huang SC, Pan ZJ, Fu CH, Chen WH, Tsai WC, and Chen HH. 2011. Gene
521 discovery using next-generation pyrosequencing to develop ESTs for *Phalaenopsis*
522 orchids. *BMC Genomics* 12:360. 10.1186/1471-2164-12-360
- 523 Hsu H-F, Hsu W-H, Lee Y-I, Mao W-T, Yang J-Y, Li J-Y, and Yang C-H. 2015. Model for
524 perianth formation in orchids. *Nature Plants* 1. 10.1038/nplants.2015.46
525 <http://www.nature.com/articles/nplants201546#supplementary-information>
- 526 Huang JZ, Lin CP, Cheng TC, Chang BC, Cheng SY, Chen YW, Lee CY, Chin SW, and Chen FC.
527 2015. A de novo floral transcriptome reveals clues into *Phalaenopsis* orchid flower
528 development. *PLoS One* 10:e0123474. 10.1371/journal.pone.0123474
- 529 Jaillon O, Aury JM, Noel B, Policriti A, Clepet C, Casagrande A, Choisne N, Aubourg S, Vitulo
530 N, Jubin C, Vezzi A, Legeai F, Huguency P, Dasilva C, Horner D, Mica E, Jublot D,
531 Poulain J, Bruyere C, Billault A, Segurens B, Gouyvenoux M, Ugarte E, Cattonaro F,
532 Anthouard V, Vico V, Del Fabbro C, Alaux M, Di Gaspero G, Dumas V, Felice N, Paillard
533 S, Juman I, Moroldo M, Scalabrin S, Canaguier A, Le Clainche I, Malacrida G, Durand E,
534 Pesole G, Laucou V, Chatelet P, Merdinoglu D, Delledonne M, Pezzotti M, Lecharny A,
535 Scarpelli C, Artiguenave F, Pe ME, Valle G, Morgante M, Caboche M, Adam-Blondon
536 AF, Weissenbach J, Quetier F, and Wincker P. 2007. The grapevine genome sequence
537 suggests ancestral hexaploidization in major angiosperm phyla. *Nature* 449:463-467.
538 10.1038/nature06148
- 539 Kanehisa M, Goto S, Sato Y, Furumichi M, and Tanabe M. 2012. KEGG for integration and
540 interpretation of large-scale molecular data sets. *Nucleic Acids Res* 40:D109-114.

- 541 10.1093/nar/gkr988
- 542 Li L, Stoeckert CJ, Jr., and Roos DS. 2003. OrthoMCL: identification of ortholog groups for
543 eukaryotic genomes. *Genome Res* 13:2178-2189. 10.1101/gr.1224503
- 544 Lin S, Lee HC, Chen WH, Chen CC, Kao YY, Fu YM, Chen YH, Lin TY. 2001. Nuclear DNA
545 contents of *Phalaenopsis* sp. and *Doritis pulcherrima*. *J Amer Soc Hort Sc.* **126**: 195-199.
- 546 Messenguy F, and Dubois E. 2003. Role of MADS box proteins and their cofactors in
547 combinatorial control of gene expression and cell development. *Gene* 316:1-21.
- 548 Mondragon-Palomino M, and Theissen G. 2011. Conserved differential expression of paralogous
549 DEFICIENS- and GLOBOSA-like MADS-box genes in the flowers of Orchidaceae:
550 refining the 'orchid code'. *Plant J* 66:1008-1019. 10.1111/j.1365-313X.2011.04560.x
- 551 Mouradov A, Cremer F, and Coupland G. 2002. Control of flowering time: interacting pathways
552 as a basis for diversity. *Plant Cell* 14 Suppl:S111-130.
- 553 Munster T, Pahnke J, Di Rosa A, Kim JT, Martin W, Saedler H, and Theissen G. 1997. Floral
554 homeotic genes were recruited from homologous MADS-box genes preexisting in the
555 common ancestor of ferns and seed plants. *Proc Natl Acad Sci U S A* 94:2415-2420.
- 556 Mutasa-Gottgens E, and Hedden P. 2009. Gibberellin as a factor in floral regulatory networks. *J*
557 *Exp Bot* 60:1979-1989. 10.1093/jxb/erp040
- 558 Parenicova L, de Folter S, Kieffer M, Horner DS, Favalli C, Busscher J, Cook HE, Ingram RM,
559 Kater MM, Davies B, Angenent GC, and Colombo L. 2003. Molecular and phylogenetic
560 analyses of the complete MADS-box transcription factor family in Arabidopsis: new
561 openings to the MADS world. *Plant Cell* 15:1538-1551.
- 562 Rudall PJ, and Bateman RM. 2002. Roles of synorganisation, zygomorphy and heterotopy in
563 floral evolution: the gynostemium and labellum of orchids and other lilioid monocots.
564 *Biol Rev Camb Philos Soc* 77:403-441.
- 565 Su CL, Chao YT, Alex Chang YC, Chen WC, Chen CY, Lee AY, Hwa KT, and Shih MC. 2011.
566 De novo assembly of expressed transcripts and global analysis of the *Phalaenopsis*
567 aphrodite transcriptome. *Plant Cell Physiol* 52:1501-1514. 10.1093/pcp/pcr097
- 568 Su CL, Chen WC, Lee AY, Chen CY, Chang YC, Chao YT, and Shih MC. 2013. A modified
569 ABCDE model of flowering in orchids based on gene expression profiling studies of the
570 moth orchid *Phalaenopsis aphrodite*. *PLoS One* 8:e80462. 10.1371/journal.pone.0080462
- 571 Tamura K, Peterson D, Peterson N, Stecher G, Nei M, and Kumar S. 2011. MEGA5: molecular
572 evolutionary genetics analysis using maximum likelihood, evolutionary distance, and
573 maximum parsimony methods. *Mol Biol Evol* 28:2731-2739. 10.1093/molbev/msr121
- 574 Theissen G. 2001. Development of floral organ identity: stories from the MADS house. *Curr*
575 *Opin Plant Biol* 4:75-85.
- 576 Trapnell C, Pachter L, and Salzberg SL. 2009. TopHat: discovering splice junctions with RNA-
577 Seq. *Bioinformatics* 25:1105-1111. 10.1093/bioinformatics/btp120

- 578 Trapnell C, Roberts A, Goff L, Pertea G, Kim D, Kelley DR, Pimentel H, Salzberg SL, Rinn JL,
579 and Pachter L. 2012. Differential gene and transcript expression analysis of RNA-seq
580 experiments with TopHat and Cufflinks. *Nat Protoc* 7:562-578. 10.1038/nprot.2012.016
- 581 Trobner W, Ramirez L, Motte P, Hue I, Huijser P, Lonng WE, Saedler H, Sommer H, and
582 Schwarz-Sommer Z. 1992. GLOBOSA: a homeotic gene which interacts with
583 DEFICIENS in the control of *Antirrhinum* floral organogenesis. *EMBO J* 11:4693-4704.
- 584 Tsai WC, Fu CH, Hsiao YY, Huang YM, Chen LJ, Wang M, Liu ZJ, and Chen HH. 2013.
585 OrchidBase 2.0: comprehensive collection of Orchidaceae floral transcriptomes. *Plant*
586 *Cell Physiol* 54:e7. 10.1093/pcp/pcs187
- 587 Tsai WC, Kuoh CS, Chuang MH, Chen WH, and Chen HH. 2004. Four DEF-like MADS box
588 genes displayed distinct floral morphogenetic roles in *Phalaenopsis* orchid. *Plant Cell*
589 *Physiol* 45:831-844. 10.1093/pcp/pch095
- 590 Tsai WC, Lee PF, Chen HI, Hsiao YY, Wei WJ, Pan ZJ, Chuang MH, Kuoh CS, Chen WH, and
591 Chen HH. 2005. PeMADS6, a GLOBOSA/PISTILLATA-like gene in *Phalaenopsis*
592 *equestris* involved in petaloid formation, and correlated with flower longevity and ovary
593 development. *Plant Cell Physiol* 46:1125-1139. 10.1093/pcp/pci125
- 594 Wang Y-T. 1995. *Phalaenopsis* Orchid Light Requirement during the Induction of Spiking.
595 *HortScience* 30:59-61.
- 596 Zerbino DR, and Birney E. 2008. Velvet: algorithms for de novo short read assembly using de
597 Bruijn graphs. *Genome Res* 18:821-829. 10.1101/gr.074492.107
- 598
- 599

Figure 1 (on next page)

Figure 1

Figure 1. Venn diagram showing unique and shared gene families between and among *Phalaenopsis*, *Oryza*, *Arabidopsis* and *Vitis*.

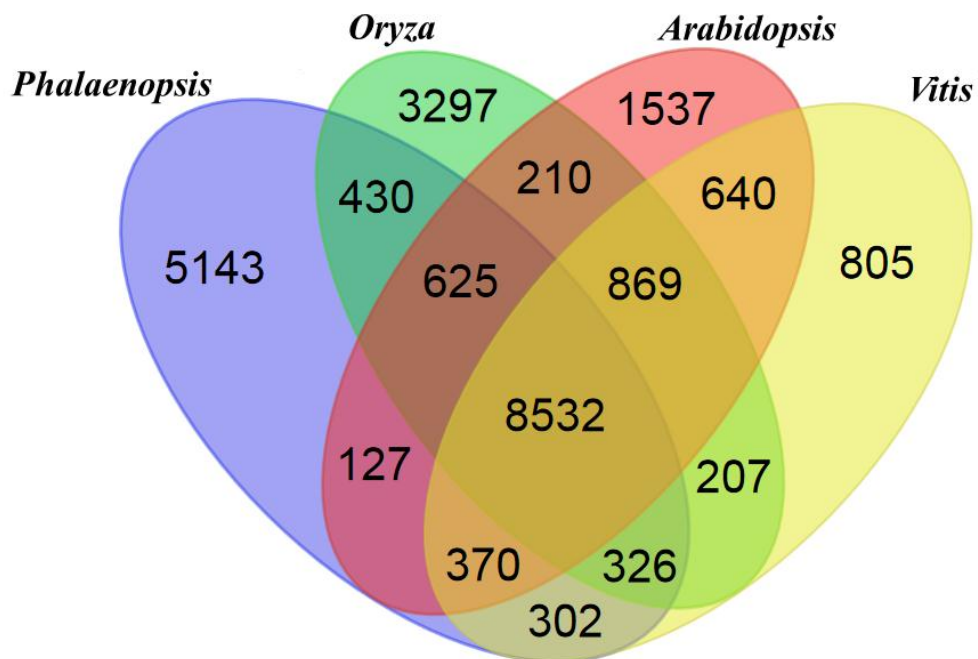
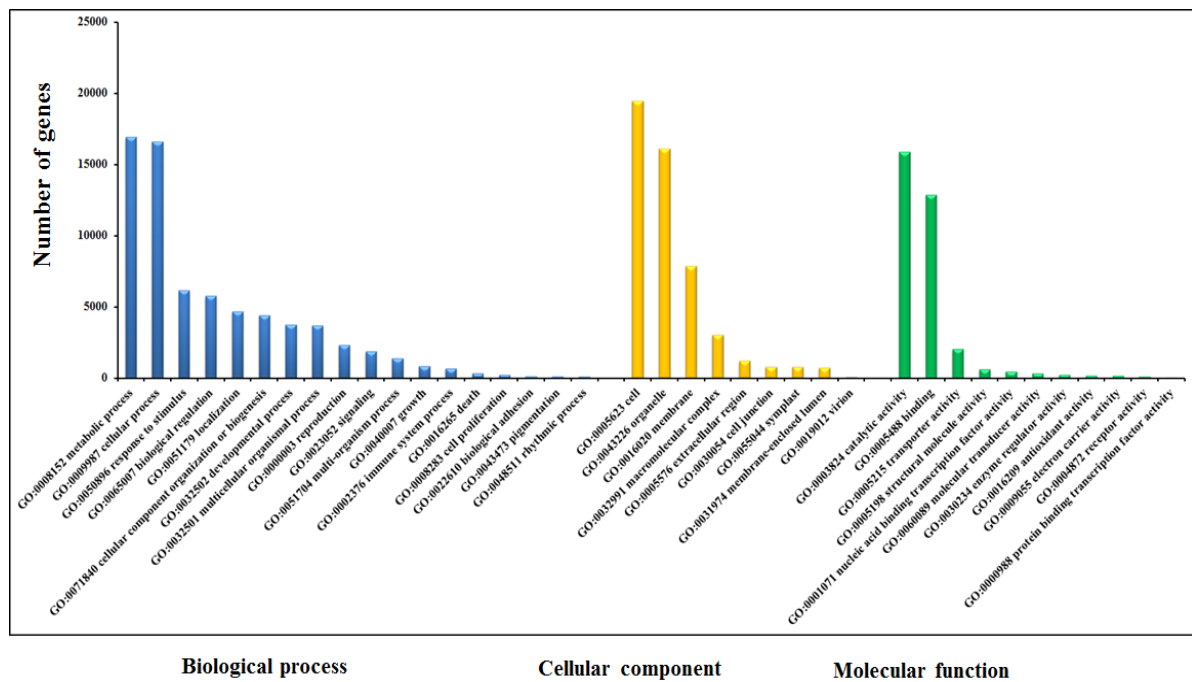


Figure 2 (on next page)

Figure 2

Figure 2. GO (A) and Pfam (B) annotation of Phalaenopsis protein-coding genes

A



B

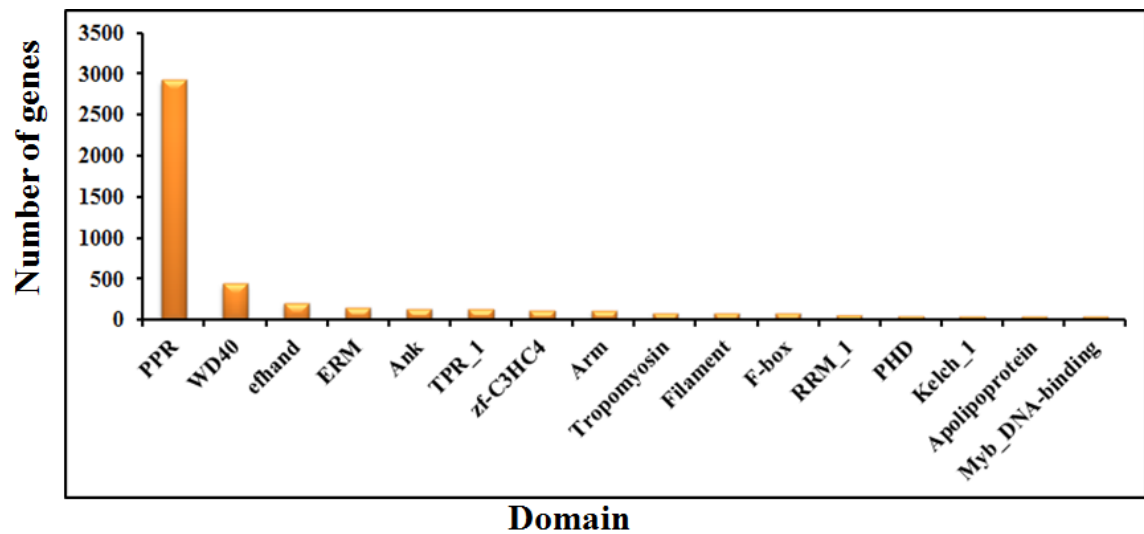


Figure 3 (on next page)

Figure 3

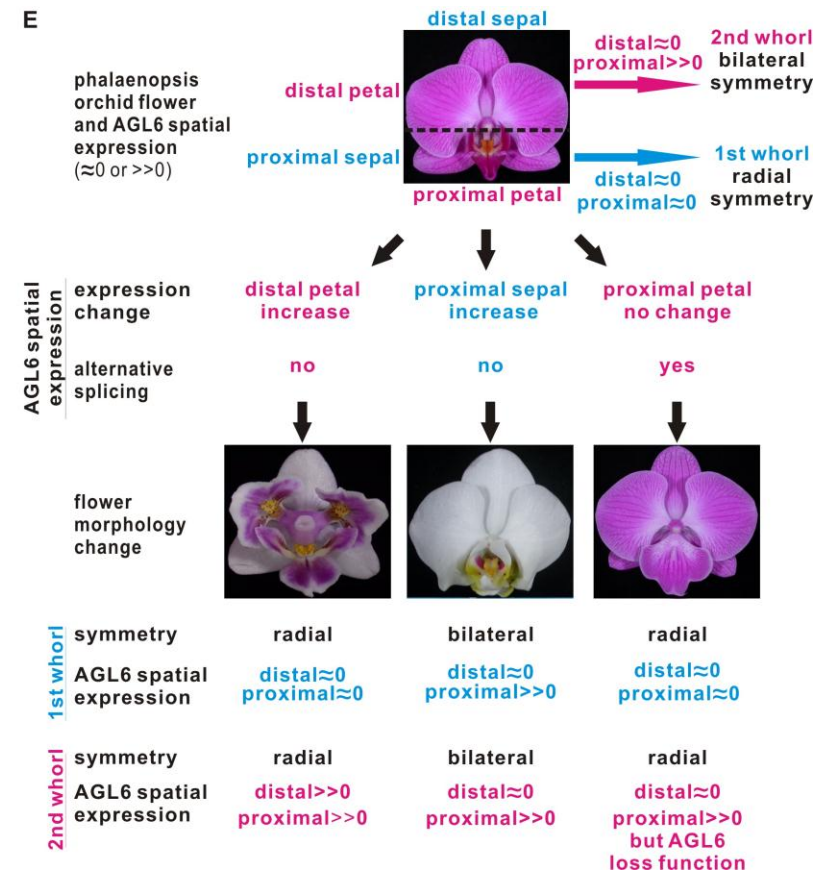
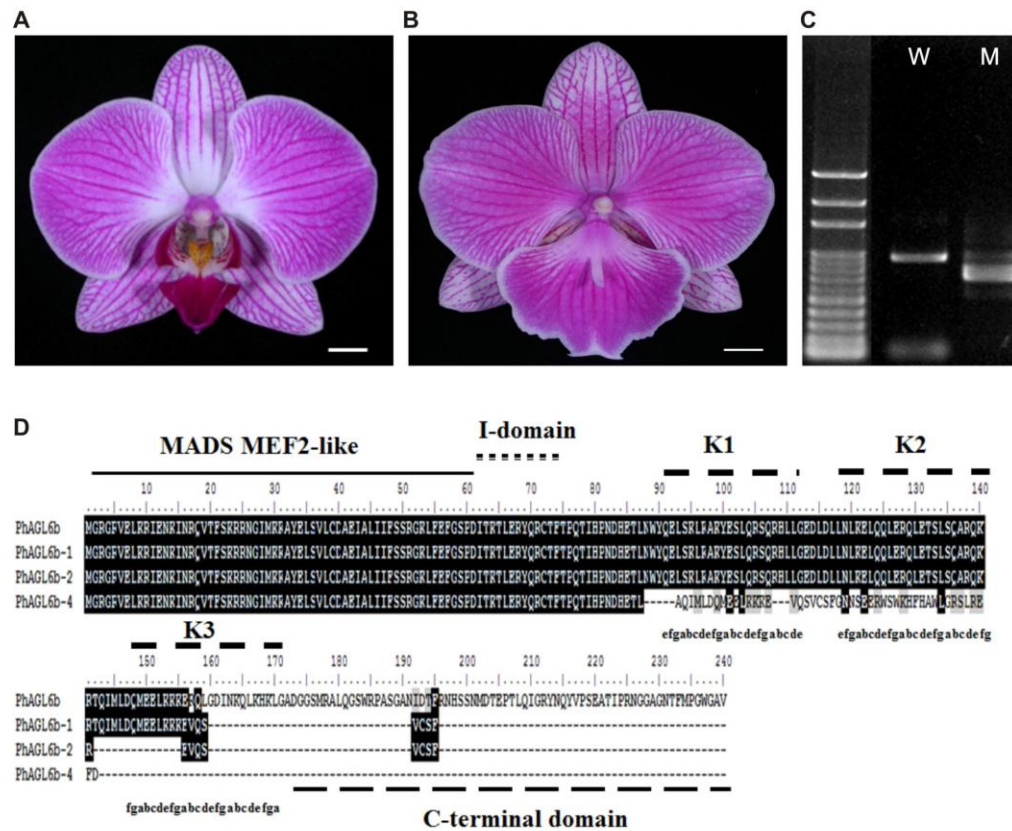
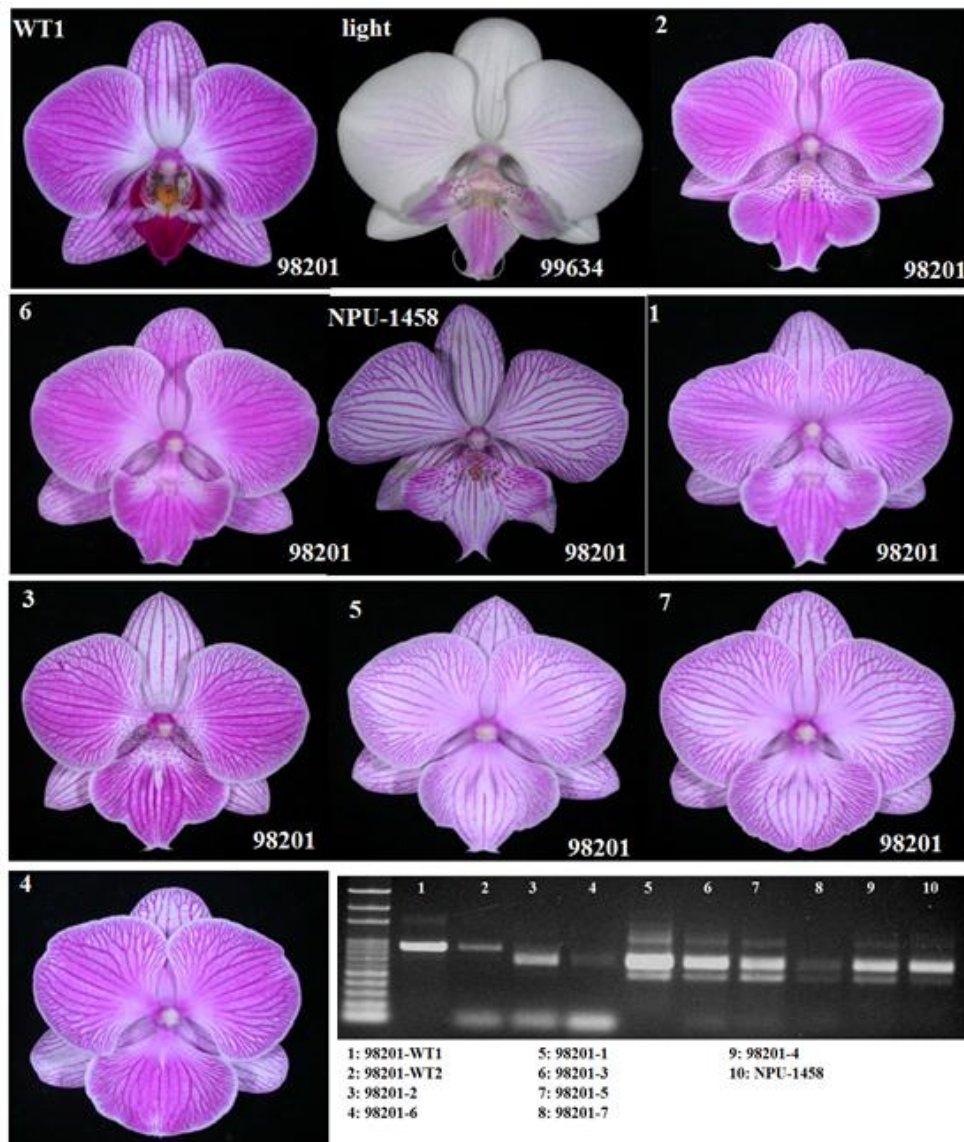


Figure 4 (on next page)

Figure 4

Figure 4. Different labellum types of wild-type and big lip mutant *Phalaenopsis* flowers. RT-PCR analysis of the mRNA splicing pattern of *PhAGL6b* in wild-type plants (98201-WT1 and 98201-WT2) and different big lip mutant types (A). Splicing variants of *PhAGL6b*, as detected via qRT-PCR in the labellum organ of different big lip mutant types (B).

A



B

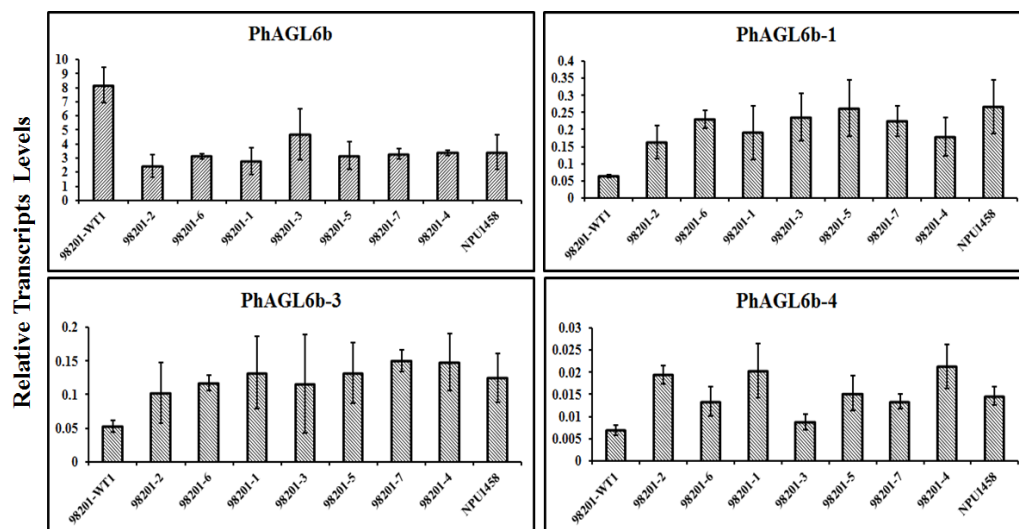


Figure 5 (on next page)

Figure 5

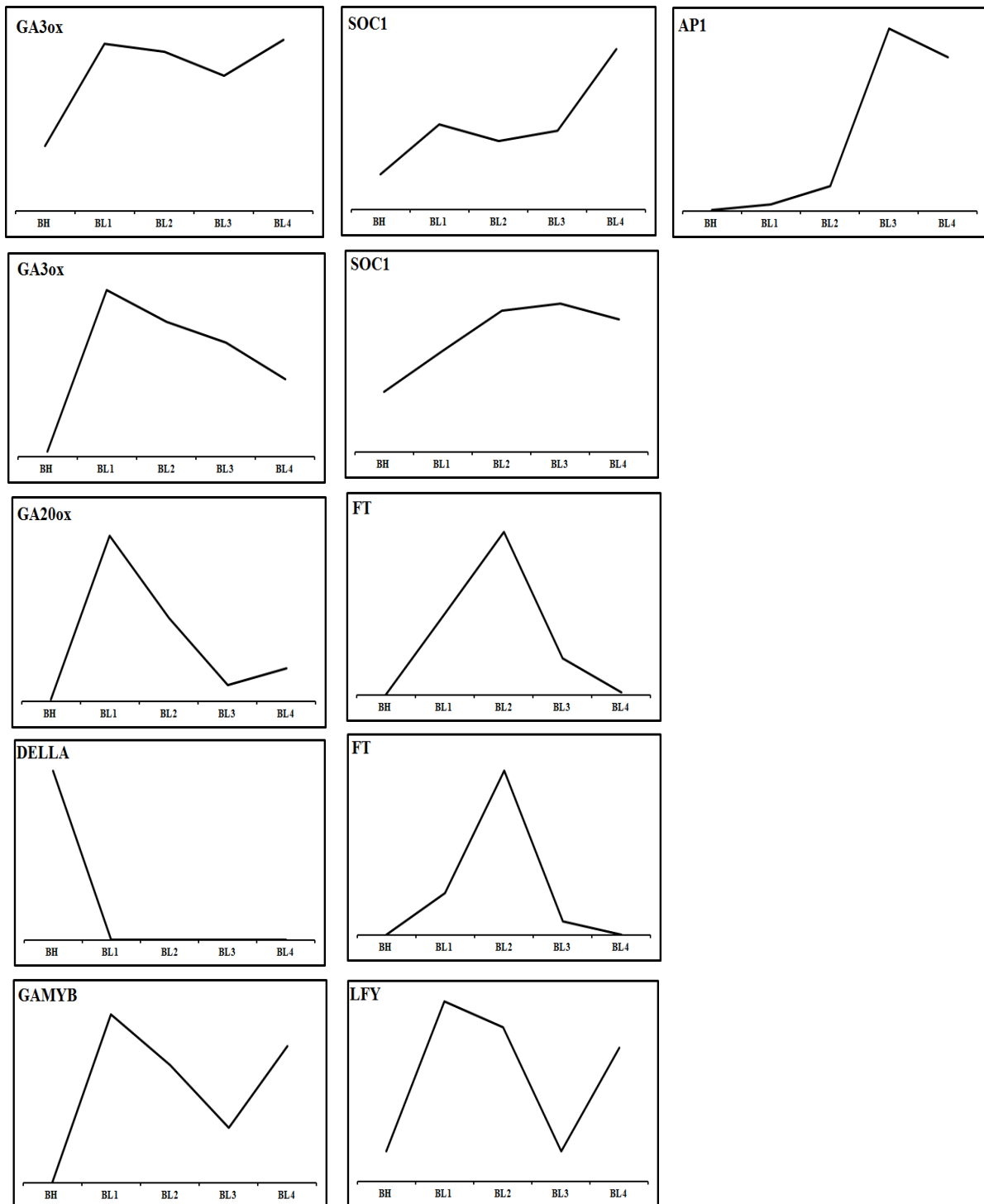


Figure 6 (on next page)

Figure 6

Figure 6. Predicted pathway in the regulation of spike induction in *Phalaenopsis*.

Red color indicates that the involved genes are more highly expressed in the GA biosynthesis pathway; whereas pink color of gene names indicates their differential expression in the GA response pathway. Blue colors of gene names represent the activation of flower architecture genes. Red arrows show the steps of the GA signaling stage; Pink arrows direct the steps of inflorescence evocation stage; Blue arrows reveal the steps of flower stalk initiation stage. Black arrows indicate the genes downregulated 2X over. *GA20ox*, *GA3ox*, *GAMYB*, *FT*, *SOC1*, *LFY* and *AP1* are upregulated 2X over.

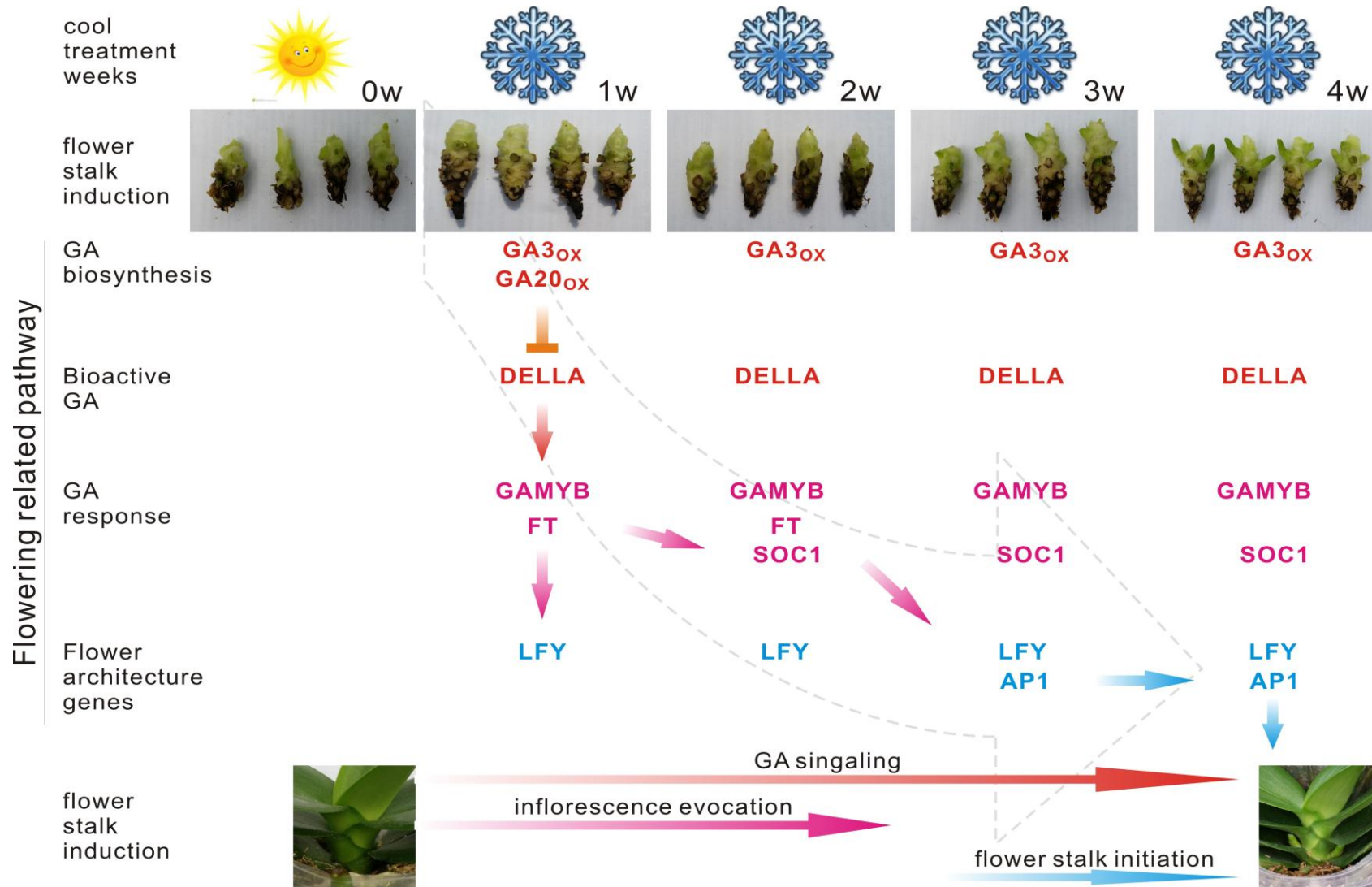


Table 1 (on next page)

Table 1

1 **Table 1 Statistics of the *Phalaenopsis* draft genome**

2	Estimate of genome size	3.45 Gb
3	Chromosome number (2n)	38
4	Total size of assembled contigs	3.1 Gb
5	Number of contigs (≥ 1kp)	630,316
6	Largest contig	50,944
7	N50 length (contig)	1,489
8	Number of scaffolds (≥ 1kp)	149,151
9	Total size of assembled scaffolds	3,104,268,398
10	N50 length (scaffolds)	100,943
11	Longest scaffold	1,402,447
12	GC content	30.7
13	Number of gene models	41,153
14	Mean coding sequence length	1,014 bp
15	Mean exon length/ number	264 bp / 3.83
16	Mean intron length/ number	3,099 bp / 2.83
17	Exon GC (%)	41.9
18	Intron GC (%)	16.1
19	Number of predicted miRNA genes	650
20	Total size of transposable elements	1,598,926,178

21

22

23

24